Theoretical Formalism for Kinesin Motility I. Bead Movement Powered by Single One-Headed Kinesins

Yi-der Chen
Mathematical Research Branch, National Institute of Diabetes and Digestive and Kidney Diseases, National Institutes of Health, Bethesda, Maryland 20892-2690 USA

ABSTRACT The directional movement on a microtubule of a plastic bead connected elastically to a single one-headed kinesin motor is studied theoretically. The kinesin motor can bind and unbind to periodic binding sites on the microtubule and undergo conformational changes while catalyzing the hydrolysis of ATP. An analytic formalism relating the dynamics of the bead and the ATP hydrolysis cycle of the motor is derived so that the calculation of the average velocity of the bead can be easily carried out. The formalism was applied to a simple three-state biochemical model to investigate how the velocity of the bead movement is affected by the external load, the diffusion coefficient of the bead, and the stiffness of the elastic element connecting the bead and the motor. The bead velocity was found to be critically dependent on the diffusion coefficient of the bead and the stiffness of the elastic element. A linear force-velocity relation was found for the model no matter whether the bead velocity was modulated by the diffusion coefficient of the bead or by the externally applied load. The formalism should be useful in modeling the mechanisms of chemimechanical coupling in kinesin motors based on in vitro motility data.

INTRODUCTION

Kinesins are microtubule-based motor proteins that can utilize the free energy of ATP hydrolysis to carry or move a cargo unidirectionally along a protofilament of a microtubule and have been found to be involved in many important processes essential for the survival of eukaryotic cells (Schroer and Sheetz, 1991; Goldstein, 1993; Barton and Goldstein, 1996; More and Endow, 1996; Hirokawa, 1998; Hamm-Alvarez and Sheetz, 1998). Since first discovered in mid-1980s, the kinesin has been found to exist as a large superfamily containing members that move toward the microtubule plus-end and members that move toward the minus-end (Golstein, 1993; Vale and Fletterick, 1997). Most intact kinesin molecules are "two-headed" dimers made of two identical heavy and two identical light chains (Vale and Fletterick, 1997). But one-headed monomeric kinesins have also been found in nature (Nangaku et al., 1994; Noda et al., 1995). The head contains both binding sites for ATP and microtubule and is the "motor" of the kinesin molecule (Vale and Fletterick, 1996; Block, 1998). Recently, the crystal structures (Kull et al., 1996; Sablin et al., 1996, 1998) and the biochemical properties (Hackney, 1996; Ma and Taylor, 1997a,b; Pechatnikova and Taylor, 1997) of some kinesin motors have been determined. However, exactly how kinesin motors convert the chemical free energy of ATP hydrolysis into mechanical work in cells is still not clear, because motility measurements in vivo are not available yet.

In contrast, motility assays involving purified kinesin motors have been developed in several laboratories (Howard et al., 1989; Block et al., 1990; Hunt et al., 1994; Svoboda and Block, 1994; Meyhofer and Howard, 1995; Vale et al., 1996; Schnitzer and Block, 1997; Wei et al., 1997). Mechanical properties, such as the step size, the force-velocity curve, etc., have been obtained for some kinesin motors. With these data, modeling on the coupling mechanism of kinesin motors can be carried out quantitatively (Duke and Leibler, 1996). However, to carry out a quantitative model calculation, one needs a procedure or formalism for calculating the mechanical movement of the motor from the parameters of the model. Previous model calculations on kinesin motors have relied on the Monte Carlo method (Chen and Hill, 1988; Leibler and Huse, 1993; Duke and Leibler, 1996). In this series of studies, we show that analytical formalisms for evaluating the motility of single motors can be obtained for a number of in vitro assays. As a result, systematic model simulations are easy to carry out. At first, we consider the assay shown in Fig. 1 where a bead is connected through an elastic element to a single motor. In this paper, the motor is assumed to have only one head. The two-headed case will be presented in another report. We were interested in this one-headed case because it has been studied experimentally (Berliner et al., 1995). Furthermore, monomeric one-headed kinesins have indeed been found in nature (Nangaku et al., 1994; Noda et al., 1995). The formalism derived here can be applied directly to these motors. In addition to the derivation of the formalism, we also apply the formalism to a simple three-state ATPase model to study how the movement of the bead is affected by the externally applied load, the diffusion coefficient of the bead, and the stiffness of the elastic element connecting the bead and the motor.

Received for publication 29 March 1999 and in final form 7 October 1999.
Address reprint requests to Dr. Yi-der Chen, NIH, Mathematical Research Branch, NIDDK, 9190 Rockville Pike, BSA Building, Suite 350, Bethesda, MD 20892-2690. Tel.: 301-496-5436; Fax: 301-402-0535; E-mail: ydchen@helix.nih.gov.

0006-3495/00/01/313/09 $2.00

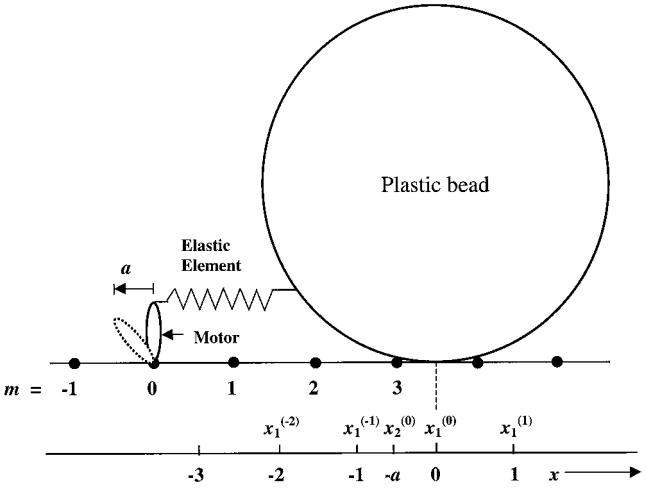

FIGURE 1 Schematic drawing of the motility assay system. The bead is connected through an elastic element to a motor, which can bind (and unbind) to a linear lattice with regularly spaced binding sites labeled as $m = 0, \pm1, \pm2, \ldots$. The motor can attach to a lattice site in two conformations, the perpendicular (state 1) and the tilted (state 2). The origin of the x axis is defined as the position of the bead when the motor is attached perpendicularly to the lattice at $m = 0$ and the elastic element is relaxed. $x_i^{(m)}$ denotes the position of the bead when the motor is attached strainlessly to site m in state i, and a is the length increase of the elastic element when the motor changes state from 1 to 2. Both x and a are made dimensionless by dividing by the length of the period of the lattice (L) which is equal to 8 nm. In this case, we have $x_1^{(m)} = m$ and $x_2^{(m)} = m - a$. The positions of some of the $x_1^{(m)}$ and $x_2^{(m)}$ on the x axis are shown explicitly.

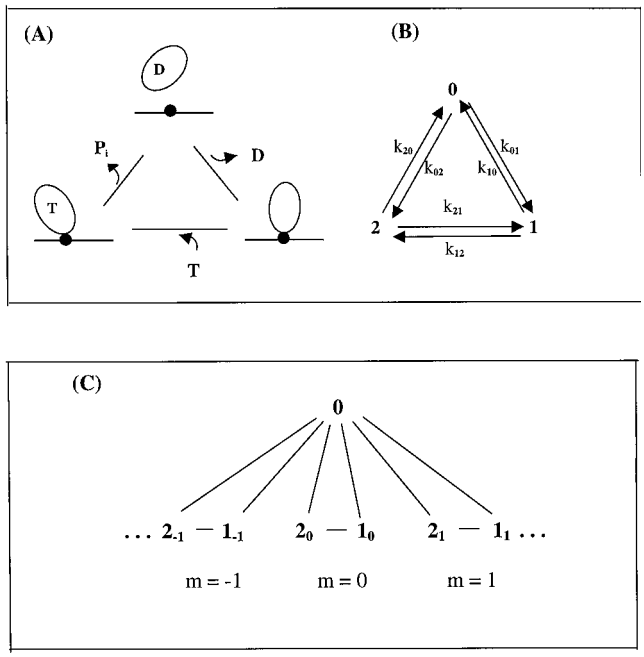

FIGURE 2 (*A*) The hypothetical three-state biochemical cycle of the ATP hydrolysis used in this study. *T*, *D*, and P_i denote ATP, ADP, and pyrophosphate, respectively. State 0 has one ADP bound and is detached from the binding site, state 1 has no bound nucleotide and is attached to the microtubule in a perpendicular conformation, and state 2 has one bound ATP and is attached to microtubule in a tilted conformation. For each clockwise cycle completion, one molecule of ATP is hydrolyzed. (*B*) The cycle diagram with the pseudo-first-order rate constants k_{ij}. Table 1 lists the values of the k_{ij} used in the calculations. (*C*) The ATP hydrolysis kinetic diagram of the motor attached elastically to a large bead as shown in Fig. 1. The detached state is represented by 0. The subscript m in 1_m and 2_m refers to the index number of the lattice site where the motor is attached (in 90° and 45° states, respectively). The same diagram is assumed to exist for each x value.

MATHEMATICAL FORMALISM

The one-headed motor is a microtubule-activated enzyme that catalyzes the hydrolysis of ATP (ATP $\rightarrow$ ADP + P_i). That is, in some intermediate states of the catalytic cycle, the motor can bind to one of the periodic binding sites on a linear protofilament (represented as a linear lattice in Fig. 1) of a microtubule. When bound to the binding site, the motor is assumed to exist in a number of conformational states, depending on the nucleotide on the motor. For simplicity we consider the simple three-state model shown in Fig. 2 *A*. In state 0, the motor has one ADP bound and is detached from the microtubule. The motor is attached to the microtubule when it is in the other two states. In state 1 the motor has no bound nucleotide and is attached perpendicularly to the lattice (the 90° state) and in state 2 the motor has one ATP bound and is attached to the lattice with a tilt to the left (the 45° state). Thus, when a cycle is completed in the clockwise direction, a molecule of ATP is hydrolyzed and a leftward swing (the "power stroke") of the axis of the bound motor is generated. If the motor is attached elastically to a bead as shown in Fig. 1, the swing motion of the motor will induce the bead to move. This is how ATP hydrolysis is coupled to mechanical movement.

When attached elastically to a large bead, the motor can still bind and unbind to the microtubule and undergo the same catalytic cycle as in Fig. 2 *A*, but the reactions will be strain-dependent. As shown in Fig. 1, we arbitrarily label the periodic lattice sites as $m = 0, \pm1, \pm2 \ldots$. The *origin* ($x = 0$) of the x axis is then defined as the *position of the bead* when the motor in state 1 (the 90° state) can attach to the site at $m = 0$ without generating any strain in the elastic element (i.e., the elastic element is relaxed). That is, the origin of the x axis is determined by the position of the site assigned as $m = 0$ and the resting length of the elastic element. The coordinate of each lattice site on this x axis will depend on the length of the elastic element, but this information is not needed in the formalism. In general, the motor can bind to more than one possible binding site. Thus, for a bead located at x, the complete kinetic diagram of the motor can be shown generally as in Fig. 2 *C*, in which 1_m represents that the motor is in state 1 (the 90° state) and is attached to the lattice site m. The motor still undergoes cyclic ATP hydrolysis reactions and conformational transformations at each m value. However, in contrast to the free motor case, the rate constants of the cycle at each m are no

longer constant, but x-dependent. When the motor is in state 1_m or 2_m (for any m), a force may be generated between the bead and the lattice, depending on whether the elastic element is strained or not.

Let us assume that the elastic element between the motor and the bead obeys Hooke's law. Then, the strain energy generated by the elastic element when the bead is at x and the motor is in state i_m can be expressed generally as

$$E_i^{(m)}(x) = \frac{z_i K}{2}(x - x_i^{(m)})^2, \quad i = 0, 1, 2, \tag{1}$$

where K is the stiffness of the elastic element, z_i is a constant equal to one or zero depending on whether the motor is attached to the lattice or not (i.e., $z_0 = 0$ and $z_1 = z_2 = 1$), and $x_i^{(m)}$ is the coordinate of the bead when the motor is attached to the lattice site m in state i ($i = 1$ or 2 only) and the elastic element is relaxed. For convenience, the quantities $E_i^{(m)}$ and x are made dimensionless by dividing their physical quantities by k_BT and L, respectively: $E_i^{(m)}(x) = \bar{E}_i^{(m)}(x)/k_BT$ and $x = \bar{x}/L$ where k_B is the Boltzmann constant, T is the absolute temperature, and L is the length of the lattice spacing (the length of a tubulin dimer in a microtubule protofilament). In this case, K is also dimensionless and is related to its corresponding physical quantity $\bar{K}$ as $K = \bar{K}L^2/k_BT$. It is easy to show that in this normalized x coordinate system $x_1^{(m)} = m$ and $x_2^{(m)} = m - a$, where a is the length increase (also in units of L) of the elastic element when the motor changes from state 1 to state 2 as shown in Fig. 1. The dimensionless force experienced by the bead at x when the motor is in state i_m is equal to

$$F_i^{(m)}(x) = z_i K(x - x_i^{(m)}) \tag{2}$$

which is related to the actual force $\bar{F}_i^{(m)}$ as $\bar{F}_i^{(m)} = F_i^{(m)}L/k_BT$.

Let k_{ij} represent the rate constant of the transition from state i to j for a motor in solution as shown in Fig. 2 *B*. Then the rate constants between states i_m and j_m in Fig. 2 *C* can be expressed generally as

$$\bar{\alpha}_{ij}^{(m)}(x) = k_{ij}\exp[\delta(E_i^{(m)}(x) - E_j^{(m)}(x))], \tag{3}$$

$$\bar{\alpha}_{ji}^{(m)}(x) = k_{ji}\exp[-(1 - \delta)(E_i^{(m)}(x) - E_j^{(m)}(x))], \tag{4}$$

where δ is a constant between 0 and 1 that determines the division of the elastic strain effect between the forward and the backward rate constants. In the calculations shown below, the value of δ is set to 0.5.

Now consider the system in Fig. 1 in which a constant external load ($\bar{F}$) is applied to the bead in the positive x direction. Let $p_0(x, t)$ be the probability of finding the bead at x and time t when the motor is in state 0 (unattached) and $p_i^{(m)}(x, t)$ ($i = 1, 2$) be the probabilities of finding the bead at x and time t when the motor is in state i_m. Then, these probabilities obey the diffusion-reaction equations (Zhou and Chen, 1996):

$$\frac{\partial p_0(x, t)}{\partial t} = -\frac{\partial u_0}{\partial x} + \sum_{i\neq 0}\sum_m \alpha_{i0}^{(m)}(x)p_i^{(m)}(x, t) - \sum_{i\neq 0}\sum_m \alpha_{0i}^{(m)}(x)p_0(x, t), \tag{5}$$

$$\frac{\partial p_i^{(m)}(x, t)}{\partial t} = -\frac{\partial u_i^{(m)}}{\partial x} + \alpha_{0i}^{(m)}(x)p_0(x, t) + \sum_{j\neq i}\alpha_{ji}^{(m)}(x)p_j^{(m)}(x, t) - \alpha_{i0}^{(m)}(x)p_i^{(m)}(x, t) - \sum_{j\neq i}\alpha_{ij}^{(m)}(x)p_i^{(m)}(x, t), \quad (i, j = 1, 2; \quad m = 0, \pm 1, \pm 2, \ldots) \tag{6}$$

where

$$u_0 = -\frac{\partial p_0}{\partial x} - Fp_0, \tag{7}$$

$$u_i^{(m)} = -\frac{\partial p_i^{(m)}}{\partial x} - p_i^{(m)}\frac{\partial E_i^{(m)}}{\partial x} - Fp_i^{(m)}, \tag{8}$$

$$\alpha_{ij}^{(m)}(x) = \bar{\alpha}_{ij}^{(m)}(x)L^2/D, \tag{9}$$

$$F = \bar{F}L/k_BT. \tag{10}$$

The D in Eq. 9 is the diffusion coefficient of the bead (not the motor!). Note that F and $\alpha_{ij}^{(m)}$ are also dimensionless.

Summing Eq. 6 over m and i and adding the sum to Eq. 5, we get $\partial p(x, t)/\partial t = -\partial u/\partial x$, where $p \equiv p_0 + \Sigma_m(p_1^{(m)} + p_2^{(m)})$ and $u \equiv u_0 + \Sigma_m(u_1^{(m)} + u_2^{(m)})$. Thus, at steady state, $\partial p/\partial t = 0$ and u becomes a constant independent of x. This steady state u is equal to the *mean velocity* of the movement of the bead on the periodic lattice, if the sum of the steady-state probabilities within each period is equal to unity (Zhou and Chen, 1996; Chen, 1997):

$$\int_0^1 \left\{p_0(x) + \sum_m [p_1^{(m)}(x) + p_2^{(m)}(x)]\right\}dx = 1. \tag{11}$$

Since $x_1^{(m)} = m$ and $x_2^{(m)} = m - a$, Eq. 1 implies that

$$E_i^{(m)}(x) = E_i^{(0)}(x - m). \tag{12}$$

Then, from Eqs. 3, 4, and 9, we have

$$\alpha_{ij}^{(m)}(x) = \alpha_{ij}^{(0)}(x - m); \quad (i \neq j = 0, 1, 2). \tag{13}$$

At steady state, it is also easy to show that

$$p_i^{(m)}(x) = p_i^{(0)}(x - m). \tag{14}$$

With Eqs. 12–14, the differential equations in Eqs. 5 and 6 at *steady state* can be reduced to the following three ordi-

nary differential equations:

$$\frac{d^2p_0(x)}{dx^2} + \sum_{i\neq 0}\sum_{m=0,\pm1,\pm2,\ldots}(\alpha_{i0}(x-m)p_i(x-m) - \alpha_{0i}(x-m)p_0(x)) = 0, \quad (15)$$

$$\frac{d^2p_i(x)}{dx^2} + \frac{d}{dx}\left[p_i(x)\left(\frac{dE_i(x)}{dx}\right)\right] + \alpha_{0i}(x)p_0(x) - \alpha_{i0}(x)p_i(x) - \sum_{j\neq i}\alpha_{ij}(x)p_i(x) + \sum_{j\neq i}\alpha_{ji}(x)p_j(x) = 0, \quad (i = 1, 2) \quad (16)$$

where the superscript (0) in $\alpha_{ij}^{(0)}$, $E_i^0(x)$, *and* $p_i^{(0)}(x)$ have been dropped for convenience. That is, the original $2(2m + 1) + 1$ equations in (5) and (6) are reduced to only three.

It is easy to show that both $\Sigma_m\ \alpha_{i0}(x - m)p_i(x - m)$ and $\Sigma_m\ \alpha_{0i}(x - m)$ in Eq. 15 are periodic in x with a period of one. As a result, $p_0(x)$ is periodic. Since the strain energy becomes very large at large x, both $p_1(x)$ and $p_2(x)$ are expected to be negligible when $|x|$ is larger than some value b. Thus, the boundary conditions for solving Eqs. 15 and 16 are:

$$p_i(-b) = p_i(b) = 0, \quad (i = 1, 2), \quad (17)$$

$$p_0(x - m) = p_0(x), \quad (m = \pm1, \pm2, \ldots). \quad (18)$$

The normalization condition in Eq. 11 becomes

$$\int_0^1 \left\{p_0(x) + \sum_m [p_1(x - m) + p_2(x - m)]\right\}dx = 1. \quad (19)$$

The differential equations in (15) and (16) with the boundary conditions in Eqs. 17–19 can be solved in the interval between $x = -b$ and $x = b$ by using the finite difference method (Zhou and Chen, 1996).

After solving the differential equations, the mean velocity of the bead u can be evaluated as

$$u = -\frac{dp_0}{dx} - Fp_0 - \sum_m\sum_{i\neq 0}\left[\frac{dp_i(x-m)}{dx} + p_i(x-m)\left\{\frac{dE_i(x-m)}{dx} + F\right\}\right]. \quad (20)$$

At steady state, the net flux of transitions between two states is the same for all three transition steps in Fig. 2 *B*. Thus, the average rate of ATP hydrolysis can be evaluated from any of the following three equations:

$$J_{01} = \int_0^1 \sum_m [\alpha_{01}(x - m)p_0(x) - \alpha_{10}(x - m)p_1(x - m)]dx \quad (21)$$

$$J_{12} = \int_0^1 \sum_m [\alpha_{12}(x - m)p_1(x - m) - \alpha_{21}(x - m)p_2(x - m)]dx, \quad (22)$$

$$J_{20} = \int_0^1 \sum_m [\alpha_{20}(x - m)p_2(x - m) - \alpha_{02}(x - m)p_0(x)]dx. \quad (23)$$

ILLUSTRATIVE CALCULATIONS

The main purpose of this paper is to derive the formalism. Therefore the following calculations are only for illustrative purpose, not for actual model fitting.

The basic parameters of the system are: 1) the diffusion coefficient D of the bead; 2) the elastic coefficient K of the elastic element; 3) the external load F applied to the bead; 4) the displacement a of the tip of the motor during the $1 \rightarrow 2$ transition; and 5) the rate constants k_{ij} of the biochemical cycle in Fig. 2 *A*. We want to study how the bead velocity and the ATP hydrolysis rate are affected by the first three parameters while keeping the last two fixed. Note that the concentrations of ATP, ADP, and P_i are defined implicitly by the values of the k_{ij} (see below) and are therefore assumed to be fixed. Table 1 lists the reference set of parameters of the model used in the calculation.

Before going into calculations, the physical meaning of some of the reference parameters in Table 1 is discussed. For a spherical bead of 100 nm in diameter (the typical size of a bead in motility assays (Wang et al., 1995)) with $D = 3 \times 10^{-10}$ cm^2/s, the viscosity of the medium as calculated from the Stokes' equation is ~0.15 poise. This is ~15 times higher than that for pure water. Since diffusion on the surface of a microtubule would be expected to be slower than diffusion in the bulk solution, this diffusion coefficient is considered as reasonable.

The dimensionless K and a are arbitrarily assigned as $K = 16$ and $a = 0.5$. Using $L = 8$ nm for the spacing

TABLE 1 The reference set of parameters used in the calculations

$D = 3 \times 10^{-9}$ cm^2/s	$K = 16.0$
$L = 8$ nm	$a = 0.5$
$k_{01} = \kappa e^{2}$	$k_{10} = \kappa e^{-2}$
$k_{12} = \kappa e^{5/2}$	$k_{21} = \kappa e^{-5/2}$
$k_{20} = \kappa e^{1/2}$	$k_{02} = \kappa e^{-1/2}$
$\kappa = 47$ s^{-1}	$\delta = 1/2$

between the two binding sites on microtubule, the actual stiffness of the elastic element at 25°C is equal to $\bar{K} = Kk_BT/L^2 = 1.035$ pN/nm. Thus, an extension of 4 nm will generate around 4 pN of force. This stiffness is roughly equal to that of a myosin cross-bridge in muscle (Brenner, 1990). The value of a is determined by the length of the motor and the degree of tilt of the motor when it changes state from 1 to 2. The length of a one-headed kinesin motor is ~6 nm. Thus, $a = 0.5$ implies that the tilt (or the swing) is ~60°. This angle is taken as the maximum swing the kinesin motor can have.

In principle, the rate constants k_{ij} of the ATPase cycle in Fig. 2 *A* should be evaluated using the measured kinetic data, such as those by Ma and Taylor (1997a). The values in Table 1 were assigned arbitrarily for simplicity. However, the thermodynamic driving force of the system and the steady-state ATP hydrolysis rate obtained using these rate constants are not unreasonable. At fixed concentrations of ATP, ADP, and P_i, the chemical driving force X defined as $X = \mu_{ATP} - \mu_{ADP} - \mu_{P_i}$ is related to the rate constants of the cycle in Fig. 2 *A* as Hill (1977):

$$e^{X/k_BT} = k_{01}k_{12}k_{20}/k_{10}k_{21}k_{02} = e^{10}. \quad (24)$$

The value of X/k_BT in real biological systems (such as in muscle) at physiological conditions is ~23 (Alberty, 1968; Eisenberg et al., 1980). That is, the concentration of ATP is assumed to be smaller than the physiological value.

The steady-state ATP hydrolysis rate (or the cycling flux) of the model in Fig. 2 *B* in the absence of the bead can be evaluated from the equation (Hill, 1977):

$$J_{ATP} = (k_{01}k_{12}k_{20} - k_{10}k_{21}k_{02})/\sum \quad (25)$$

where

$$\sum \equiv k_{21}k_{10} + k_{12}k_{20} + k_{10}k_{20} + k_{02}k_{21} + k_{20}k_{01} + k_{01}k_{21} + k_{01}k_{12} + k_{10}k_{02} + k_{12}k_{02} \quad (26)$$

With the rate constants given in Table 1, Eq. 25 gives a rate of 53.4 s^{-1}, which is very close to the experimental value of 60 s^{-1} found for one-headed kinesin motors by Ma and Taylor (1997a).

Effect of diffusion coefficient in the absence of an external load: the force-velocity curve

The mean velocity of the bead ($\bar{u}$) and the rate of the ATP hydrolysis ($\bar{J}$) calculated as a function of the diffusion coefficient D based on the parameters in Table 1 in the absence of an external load ($F = 0$) are shown in Fig. 3 *A*. Note that all the calculated quantities in the figure have been converted into real physical quantities with dimensions. As shown in the figure, both the bead velocity and the ATP hydrolysis rate decrease slightly when the diffusion coefficient of the bead is decreased from the reference value (3×10^{-9} cm^2/s): pronounced decrease in $\bar{u}$ and $\bar{J}$ occurs only after D is reduced well below 0.1×10^{-9} cm^2/s. At small D, the bead velocity is more affected by the diffusion coefficient than the ATP hydrolysis rate. The reason for the decline in the velocity at very small D is that the bead does not have enough time to respond to the conformational change of the kinesin head before it detaches. The average time for the kinesin head to remain in the attached state 2 can be estimated roughly as $[(k_{20} + k_{21})e^{Ka^2/4}]^{-1} \approx 4.5$ ms. The relaxation time of the spring can be derived as $k_BT/\bar{K}D = L^2/KD$, which yields a value of 0.013 ms at $D = 3 \times 10^{-9}$ cm^2/s. Thus, at this D value, the bead responds instantaneously to the conformational change of the kinesin head and the diffusion coefficient of the bead has little effect on the velocity of the bead. However, when the value of D is

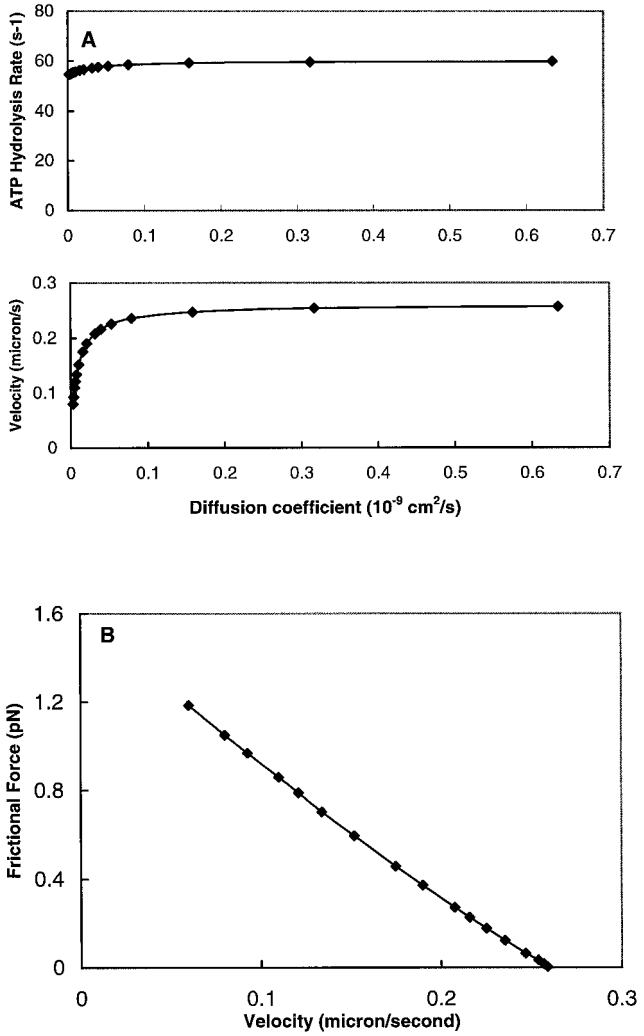

FIGURE 3 (*A*) The bead velocity and the ATP hydrolysis rate calculated as a function of the diffusion coefficient of the bead using the reference parameters listed in Table 1. (*B*) The force-velocity curve obtained by plotting the product of the velocity and the diffusion coefficient (the frictional force) as a function of the velocity.

reduced 100 times so that the spring relaxation time becomes comparable to the time of the attached kinesin head, the bead has not enough time to respond and the velocity is therefore greatly reduced.

The ATP hydrolysis rate at a fixed x can be evaluated from Eq. 25 if the k values are replaced by the strain-dependent α values of Eqs. 3 and 4. It is easy to see that the hydrolysis rate is only slightly dependent on the strain of the spring, because the strain-dependent part appears only in the Σ term, not in the numerator of the rate equation. As a result, the ATP hydrolysis rate is less dependent on D than the bead velocity as shown in Fig. 3 *A*.

The mean frictional force experienced by the bead at $\bar{u}$ is equal to $\bar{u}k_BT/D$. Thus, the force-velocity curve can be obtained easily from the velocity curve in Fig. 3 *A* and is shown in Fig. 3 *B*. The curve is almost linear. The maximum bead velocity and the maximum force obtained by extrapolation are 0.26 μ/s and 1.6 pN, respectively. The limiting velocity of the bead is close to what was measured for one-headed kinesins (Berliner et al., 1994). The value of the maximum force is smaller than that measured for the *two-headed* kinesins (Hunt et al., 1994).

Effect of external load: another force-velocity curve

By varying the value of F in Eqs. 7 and 8, the effect of a constant external load on the bead movement and the ATP hydrolysis of the system can be studied. The calculated velocity as a function of load (F) is plotted in Fig. 4 for two D values. In both cases, the load-velocity curve is linear, but the overall characteristics are quite different. For the reference D case ($D = 3 \times 10^{-9}$ cm^2/s), the maximum load at $u = 0$ is $\sim$0.017 pN. When the diffusion coefficient is reduced by 100 times, the maximum load increases $\sim$50 times to 0.8 pN. In other words, the velocity of the bead is more sensitive to the external load when the viscosity of the medium or the size of the bead is small (so that the diffusion coefficient of the bead becomes larger). This is reasonable, because the bead is easily pulled or pushed by the external load if the diffusion coefficient is large.

The decline in velocity with increasing load is a consequence of backward slippage of the bead when the kinesin head is detached. The motor stalls when the distance slipped while detached is equal to the distance moved forward while attached. The stall force at large D (the reference value) can be estimated approximately as follows. The velocity of the slippage is equal to $\bar{F}D/k_BT$. The time for the head to remain *unattached* at large D can be estimated roughly as $1/k_{01}$. The product of these two quantities is the distance of the backward slippage after one ATP hydrolysis cycle is completed. Thus, the stall force can be evaluated when this slippage distance is set equal to the forward movement distance $\bar{a}$: $\bar{F}_{stall} = aLk_{01}k_BT/D$. With the parameters of Table 1, this equation gives a stall force of 0.019 pN, which is close to

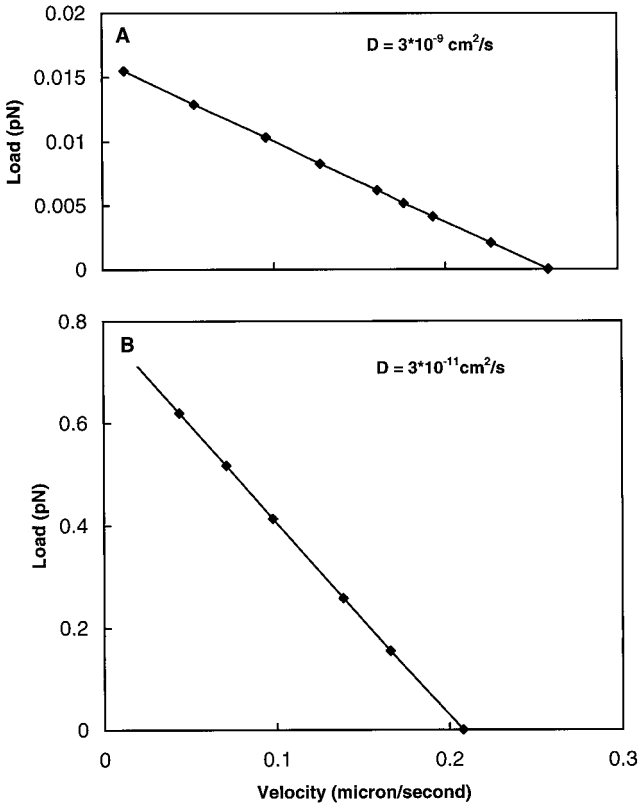

FIGURE 4 The force-velocity curves calculated as a function of the external load $\bar{F}$ for two fixed diffusion coefficients.

that shown in Fig. 4 *A*. The stall force evaluated from this equation at $D = 0.03 \times 10^{-9}$ cm^2/s is much larger than the calculated value (Fig. 4 *B*), because the time to remain unattached is overestimated.

Effect of the stiffness of the elastic element

In Fig. 5, the calculated bead velocity and the ATP hydrolysis rate of the system at $F = 0$ are plotted as a function of the stiffness of the elastic element for two values of diffusion coefficients. As shown in the figures, when the stiffness (K) of the elastic element is reduced, the ATP hydrolysis increases monotonically, while the bead velocity increases at high K, reaches a peak, and then decreases toward the zero value as K goes to zero (the peak was not obtained for the $D = 3 \times 10^{-9}$ cm^2/s case because the calculation was not carried out far enough to very small K values). The occurrence and the position of the peak in the velocity-stiffness curves can be predicted also based on the spring relaxation time of the system discussed before.

When the spring is very stiff (large K), the movement of the bead is completely coupled to the conformational change of the kinesin head. In this case, the velocity of the bead is proportional to the ATP hydrolysis rate. Since the attachment rate of the kinesin head is slightly proportional

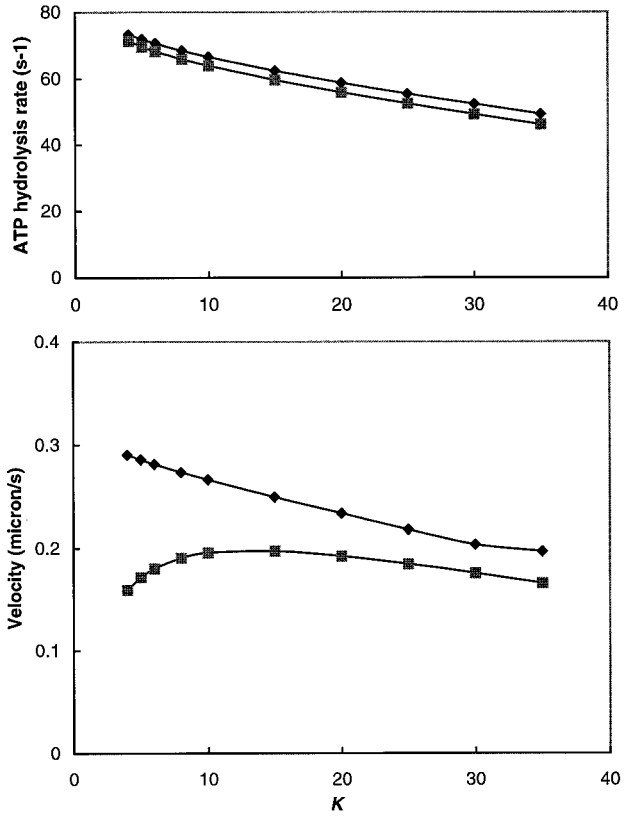

FIGURE 5 The bead velocity and the ATP hydrolysis rate of the system calculated as a function of the stiffness of the elastic element. The diffusion coefficients used in the calculations are 3×10^{-9} cm^2/s (*filled diamond*) and 0.03×10^{-9} cm^2/s (*filled square*).

to the strain of the elastic element, the ATP hydrolysis rate is expected to increase as K is reduced. So is the velocity of the bead. However, when the spring is completely flexible ($K = 0$), the velocity of the bead is expected to be zero, because the movement of the bead and the conformational change of the kinesin head are completely uncoupled. The peak of the velocity curve is expected to occur when the relaxation time of the spring is of the same order of the time of the attached state of the head. As discussed before, the time of the attached state is ~4.5 ms. Thus, the peak is estimated roughly to be around $K = 0.05$ and 5 for $D = 3 \times 10^{-9}$ cm^2/s and $D = 0.03 \times 10^{-9}$ cm^2/s, respectively.

DISCUSSION AND CONCLUSIONS

The reason that the bead in Fig. 1 can execute a net movement toward the left when the catalytic cycle in Fig. 2 *A* is favored in the clockwise direction can be explained as follows. Suppose the bead is originally at $x = 0$ and the motor is detached (state 0). When attachment occurs, the motor will attach perpendicularly (in state 1) to the lattice (because the direction of the cycle completion is $0 \rightarrow 1 \rightarrow 2 \rightarrow 0$). Then, the most probable binding site on the lattice for the motor to bind to is the site at $m = 0$ (since $x_0^{(0)} = 0$, see above and Fig. 1). As the motor changes its state from 1 to 2, a force is generated in the elastic element, which in turn will pull the bead toward the left. Thus, after the motor detaches from the lattice, the probability of rebinding the motor to the original site 0 is reduced, because the bead is now located on the left of $x_0^{(0)}$. However, the probability of binding the motor to the lattice site at $m = -1$ is now increased. Thus, after several cycles, both the motor and the bead will move together toward the left. Similarly, if the chemical transition in Fig. 2 *A* is counterclockwise (ATP is being synthesized, a process not possible in reality because the standard free energy of the ATP hydrolysis is very large), then both particles will move toward the right. It is now obvious that the presence of the bead causes the motor to diffuse and bind more favorably in one direction than the other. That is, the bead in Fig. 1 acts as a "rectifier" for the direction of the diffusion and the subsequent binding of a detached motor. For a free motor (without the bead), the diffusion of the motor to the binding sites on the lattice is not directionally biased. Therefore, no net biased movement is expected for a free one-headed motor. A recent experiment (Vale et al., 1996) indicates that this might be the case for kinesin motors. For two-headed motors, biased movement is possible even without the bead, because the head attached to the microtubule can act as the directional rectifier for the binding of the other head, as suggested in the "hand-over-hand" model for kinesin motors (Howard et al., 1989; Hackney, 1994).

We would like to point out that the direction of the movement of the bead is closely related to the sign of a (or the direction of the swing of the motor axis, see Fig. 1). In fact, it is the direction of the cycling in Fig. 2 *A* and the direction of the swing of the motor that determine the direction of the net movement of the bead. It is also important to note that this conclusion does not depend on how the bead and the motor are arranged spatially on the lattice. That is, as long as the cycling in Fig. 2 *A* is clockwise, the bead will still move to the left even when the bead is placed on the left side of the motor (opposite to that shown in Fig. 1). The exchange of the position of the bead relative to the motor simply changes the force acting on the bead from the "pull" mode into the "push" mode (or vice versa) and the net result is the same.

In in vitro motility experiments (Berliner et al., 1994), it has been found that beads attached with single one-headed kinesin motors do not move in a straight line along a single protofilament all the time; they can jump to neighboring protofilaments or diffuse away from the microtubule. This is not unexpected, since the bead can diffuse away from the microtubule when the motor is not attached to the microtubule. However, this does not diminish the usefulness of this formalism in modeling, because one can always pick up the data that show the "linear" movement behavior and use them in the analysis. Experimentally, one could increase the fraction of the linear movement of the bead by adding macromolecules to the system to increase the viscosity of

the medium and force the bead to stay longer to the protofilament (Young et al., 1998).

Although we have used the macroscopic Hooke's law to describe the elasticity of the elastic element connecting the motor to the bead, the same formalism can be derived based on statistical mechanical arguments (Hill, 1975). In fact, the overall stiffness of the system should involve contributions from the motor itself. In this case, the appropriate approach is to use the statistical mechanical formulation.

It is important to point out that the velocity of the bead in Fig. 1 calculated for the three-state model was found to depend on the stiffness of the elastic element used in the system (see Fig. 5, *bottom*). This finding implies that the value of the bead velocity measured in in vitro motility assays should depend on the length or the elasticity of the elastic element used in the experiment. We expect this conclusion to be true even when the kinetic model is more complicated than that shown in Fig. 2 *A* or even when the kinesin motor in Fig. 1 is two-headed. Even in microtubule-gliding assays (Howard et al., 1989; Berliner et al., 1994; Stewart et al., 1995), the velocity of the microtubule moving on fixed kinesin motors (one-headed or two-headed) should also depend on the length of the element attaching the motor to the surface.

We would like to point out that the force-velocity curve for the bead in Fig. 1 calculated by varying the diffusion coefficient and by varying the external load are quite different, although both curves have linear dependence. It is interesting to see whether the same result will be obtained for the bead attached with two-headed motors. Experimentally, the diffusion coefficient of the bead can be varied by varying the viscosity of the medium or the size of the bead.

In conclusion, we have developed a formalism connecting the biochemical model of the motor and the motility of the bead in a motility assay shown in Fig. 1. The formalism involves the solution of a set of coupled ordinary differential equations that can be carried out numerically using the finite difference method. Although it was derived based on a three-state model, the formalism is very general in that it can be applied to models with an arbitrary number of states in the catalytic cycle. The formalism should be very useful in modeling the mechanisms underlying the motility of biological motors based on in vitro motility data.

I thank one of the referees for his valuable discussions on the physical interpretations of the results of the illustrative calculations presented in this paper.

REFERENCES

Alberty, R. A. 1968. Effect of pH and metal ion concentrations on the equilibrium hydrolysis of adenosine triphosphate to adenosine diphosphate. *J. Biol. Chem.* 243:1337–1343.

Barton, N. R., and L. S. B. Golstein. 1996. Going motile: microtubule motors and chromosome segregation. *Proc. Natl. Acad. Sci. USA.* 93: 1735–1742.

Berliner, E., H. K. Mahtani, S. Karki, L. F. Chu, J. E. Cronan, Jr., and J. Gelles. 1994. Microtubule movement by a biotinated kinesin bound to a streptavidin-coated surface. *J. Biol. Chem.* 269:8610–8614.

Berliner, E., E. C. Younf, K. Anderson, H. K. Mahtani, and J. Gelles. 1995. Failure of a single-headed kinesin to track parallel to microtubule protofilaments. *Nature.* 373:718–721.

Block, S. M. 1998. Leading the procession: new insight into kinesin motors. *J. Cell Biol.* 140:1281–1284.

Block, S. M., L. S. B. Goldstein, and B. J. Schnapp. 1990. Bead movement by single kinesin molecules studied with optical tweezers. *Nature.* 348:348–352.

Brenner, B. 1990. Muscle mechanics and biochemical kinetics. *In* Molecular Mechanisms in Muscle Contraction. J. M. Squire, editor. CRC Press, Boca Raton, FL.

Chen, Y. 1997. Asymmetric cycling and biased movement of Brownian particles in fluctuating symmetric potentials. *Phys. Rev. Lett.* 79: 3117–3120.

Chen, Y., and T. L. Hill. 1988. Theoretical calculation methods for kinesin in fast axonal transport. *Proc. Natl. Acad. Sci. USA.* 85:431–435.

Duke, T., and S. Leibler. 1996. Motor protein mechanics: a stochastic model with minimal mechanochemical coupling. *Biophys. J.* 71: 1235–1247.

Eisenberg, E., T. L. Hill, and Y. Chen. 1980. Cross-bridge model of muscle contraction. Quantitative analysis. *Biophys. J.* 29:195–227.

Goldstein, L. S. B. 1993. With apologies to Scheherazade: tails of 1001 kinesin motors. *Annu. Rev. Genet.* 27:319–351.

Hackney, D. D. 1994. Evidence for alternating head catalysis by kinesin during microtubule-stimulated ATP hydrolysis. *Proc. Natl. Acad. Sci. USA.* 91:6865–6869.

Hackney, D. D. 1996. The kinetic cycles of myosin, kinesin, and dynein. *Annu. Rev. Physiol.* 58:731–750.

Hamm-Alvarez, S. F., and M. P. Sheetz. 1998. Microtubule-dependent vesicle transport: modulation of channel and transport activity in liver and kidney. *Physiol. Rev.* 78:1109–1129.

Hill, T. L. 1977. Free Energy Transduction in Biology. Academic Press, New York.

Hirokawa, N. 1998. Kinesin and dynein superfamily proteins and the mechanism of organelle transport. *Science.* 279:519–526.

Howard, J., A. J. Hudspeth, and R. D. Vale. 1989. Movement of microtubules by single kinesin molecules. *Nature.* 342:154–158.

Hunt, A. J., F. Gittes, and J. Howard. 1994. The force exerted by kinesin against a viscous load. *Biophys. J.* 67:766–781.

Kull, F. J., E. P. Sablin, R. Lau, R. J. Fletterick, and R. D. Vale. 1996. Crystal structure of kinesin motor domain reveals a structural similarity to myosin. *Nature.* 380:550–555.

Leibler, S., and D. A. Huse. 1993. Porters versus rowers: a unified stochastic model of motor proteins. *J. Cell Biol.* 121:1357–1368.

Ma, Y-Z., and E. W. Taylor. 1997a. Kinetic mechanism of a monomeric kinesin construct. *J. Biol. Chem.* 272:717–723.

Ma, Y-Z., and E. W. Taylor. 1997b. Interacting head mechanism of microtubule-kinesin ATPase. *J. Biol. Chem.* 272:724–730.

Meyhofer, E., and J. Howard. 1995. The force generated by a single kinesin molecule against an elastic load. *Proc. Natl. Acad. Sci. USA.* 92: 574–578.

More, J. D., and S. A. Endow. 1996. Kinesin proteins: a phylum of motors for microtubule-based motility. *Bioessays.* 18:207–219.

Nangaku, M., R. Sato-Yoshitake, Y. Okada, Y. Noda, and R. Takemura. 1994. KIF1B, a novel microtubule plus end-directed monomeric motor protein for transport of mitochondria. *Cell.* 79:1209–1220.

Noda, Y., R. Sato-Yoshtake, S. Kondo, M. Nangaku, and N. Hirokawa. 1995. KIF2 is a new microtubule-based anterograde motor that transports membraneous organelles distinct from those carried by kinesin heavy chain or KIF3A/B. *J. Cell Biol.* 129:157–167.

Pechatnikova, E., and E. W. Taylor. 1997. Kinetic mechanism of monomeric non-claret disjunctional protein (ncd) ATPase. *J. Biol. Chem.* 272:30735–30740.

Sablin, E., F. J. Kull, R. Cooke, R. D. Vale, and R. J. Fletterick. 1996. Crystal structure of the motor domain of the kinesin-related motor ncd. *Nature.* 380:555–559.

Sablin, E. P., R. B. Case, S. C. Dai, C. L. Hart, A. Ruby, R. D. Vale, and R. J. Fletterick. 1998. Direction determination in the minus-end-directed kinesin motor ncd. *Nature.* 395:813–816.

Schnitzer, M. J., and S. M. Block. 1997. Kinesin hydrolyses one ATP per 8-nm step. *Nature.* 388:386–390.

Schroer, T. A., and M. P. Scheetz. 1991. Functions of microtubule-based motors. *Annu. Rev. Physiol.* 53:629–652.

Stewart, R. J., J. Semerjian, and C. F. Schmidt. 1998. Highly processive motility is not a general feature of the kinesins. *Eur. Biophys. J.* 27: 353–360.

Svoboda, K., and S. M. Block. 1994. Force and velocity measured for single kinesin molecules. *Cell.* 77:773–784.

Vale, R. D., and R. J. Fletterick. 1997. The design plan of kinesin motors. *Annu. Rev. Cell. Biol.* 13:745–777.

Vale, R. D., T. Funatsu, D. W. Pierce, L. Romberg, Y. Harada, and T. Yanagida. 1996. Direct observation of single kinesin molecules moving along microtubules. *Nature.* 380:451–453.

Wang, Z., S. Khan, and M. P. Sheetz. 1995. Single cytoplasmic dynein molecule movements: characterization and comparison with kinesin. *Biophys. J.* 69:2011–2023.

Wei, H., E. C. Young, M. L. Fleming, and J. Gelles. 1997. Coupling of kinesin steps to ATP hydrolysis. *Nature.* 388:390–393.

Young, E. C., H. K. Mahtani, and J. Gelles. 1998. One-headed kinesin derivatives move by a nonprocessive, low-duty ratio mechanism unlike that of two-headed kinesin. *Biochemistry.* 37:3467–3479.

Zhou, H-X., and Y. Chen. 1996. Chemically driven motility of Brownian particles. *Phys. Rev. Lett.* 77:194–197.